Zero-energy proton dissociation of H_2^+ through stimulated Raman scattering

Xinhua Xie (谢新华),[1,*] Stefan Roither,[1] Seyedreza Larimian,[1] Sonia Erattupuzha,[1] Li Zhang (张丽),[1] Daniil Kartashov,[1] Feng He (何峰),[2] Andrius Baltuška,[1] and Markus Kitzler[1,†]

[1]*Photonics Institute, Technische Universität Wien, A-1040 Vienna, Austria*

[2]*Key Laboratory for Laser Plasmas (Ministry of Education) and Department of Physics, Shanghai Jiao Tong University, Shanghai 200240, People's Republic of China*

(Received 4 October 2018; revised manuscript received 14 January 2019; published 8 April 2019)

We experimentally investigate dissociation of H_2^+ in the (near-)zero proton energy region. Based on our experimental results we conclude that the underlying mechanism for the production of protons with such low energy in strong two-color and broadband laser fields is a stimulated Raman-scattering-based zero-photon-dissociation process, ZPD_{stR}, taking place on the electronic ground state. It is furthermore shown that in the (near-)zero energy region the asymmetry in proton ejection induced by asymmetric laser fields is due to the interplay of several processes, rather than only pathway interferences, with vibrational trapping (or bond hardening) taking a key role.

DOI: 10.1103/PhysRevA.99.043409

Much of our understanding used in the research on manipulating molecular reactions with strong, tailored light fields [1–5] is rooted in work done on H_2 [6–17]. Key concepts emerging from the research on H_2 are, e.g., the emergence of light-induced molecular potentials (LIPs) [18,19], bond softening via the net absorption of one [20,21], two [21,22], or more [23,24] photons, or bond hardening [25–29], also known as molecular stabilization or vibrational trapping (VT); see Refs. [18,19,30,31] for further details. However, even for this simplest of all molecules there exist still a number of issues awaiting clarification, in particular in the family of bond-hardening phenomena. Examples include direct experimental confirmation of light-induced conical intersections (LICIs) [32–35], or a generally accepted picture of the concept of trapping that has been challenged by McKenna *et al.* [36].

Here, we focus on a bond-hardening process that leads to protons with (near-)zero kinetic energy during the dissociation $H_2^+ \rightarrow H^+ + H$. This dissociation pathway was predicted [25] and observed [28] decades ago. It has been explained as bond hardening at the zero-photon crossing of the Floquet ladder through dissociation involving the net absorption of zero photons (zero-photon dissociation, ZPD) [25,27,28]. However, because during ionization of H_2 at the Franck-Condon region the probability for populating vibrational levels higher than $v = 5$ is small, it necessitates laser wavelengths $\lesssim$400 nm to efficiently drive this process [25,28]. Several recent experiments have shown that the yield of protons with (near-)zero energy increases particularly strongly when two-color laser fields are used to drive the H_2 dissociation process, e.g., Refs. [15,16,29,37–39]. But also in experiments [12,13,40] and simulations [23,24] applying few-cycle pulses with a broadband spectrum centered around 730–750 nm a notable enhancement of the (near-)zero energy proton yield was observed. The appearance of these low-energy protons in two-color fields was explained by a two-step process, where after ionization a 400-nm photon is resonantly absorbed at a stretched H-H^+ bond to transiently populate the $2p\sigma_u$ state and, subsequently, at a still further stretched bond, an 800-nm photon is emitted, returning the population to the $1s\sigma_g$ state where H_2^+ finally dissociates via the net absorption of zero photons (ZPD); see, e.g., Refs. [15,29,37,39]. To stress the involvement of the $2p\sigma_u$ state in this ZPD process, we refer to it as $ZPD_{2p\sigma_u}$ (see Fig. 1 for a visualization).

In this paper we show experimentally that the yield enhancement of protons with (near-)zero energy observed in two-color fields [15,16,29,37–39] and, with a somewhat smaller probability, also in broadband few-cycle pulses [12,13,23,24,40] is dominantly caused by a stimulated Raman scattering process, denoted by ZPD_{stR} in Fig. 1, rather than by the $ZPD_{2p\sigma_u}$ process. Our work furthermore outlines the connection between the stimulated Raman scattering process and other processes leading to low-energy protons indicated in Fig. 1, thereby filling the gaps of our thus far incomplete understanding of H_2 dissociation in this energy range.

In our experiments we employed broadband 5-fs pulses [center wavelength (CL) 740 nm] as well as narrow-band 25-fs pulses (CL 800 nm) and their frequency doubles (CL 400 nm, duration 50 fs). With the narrow-band pulses we also generated two-color fields $E(t) = E_{\omega_{800}} \cos(\omega_{800} t) + E_{\omega_{400}} \cos(\omega_{400} t + \Delta\varphi)$ with $E_{\omega_{800}} \approx E_{\omega_{400}}$ in the focus. All pulses were polarized along z. The relative phase $\Delta\varphi$ was varied using a glass wedge pair. We used a reaction microscope [41,42] to measure the three-dimensional momentum vectors of electrons and ions emerging from the interaction of H_2 molecules with the laser fields. The laser beam was focused onto an ultrasonic jet of H_2 in the interaction chamber (background pressure 1.3×10^{-10} mbar). Electrons and ions were guided by weak magnetic (6.4 G) and electric (2.5 V/cm) fields along the spectrometer axis (z direction) to two position- and time-sensitive multihit detectors situated at

*xinhua.xie@tuwien.ac.at
†markus.kitzler@tuwien.ac.at

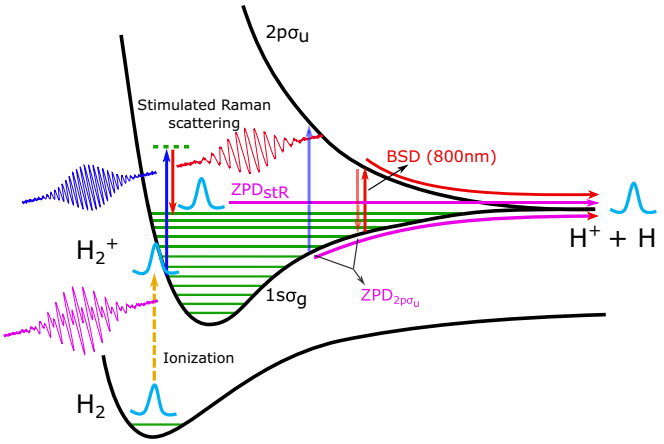

FIG. 1. Schematic of dissociation processes of H_2 relevant for the production of protons with near-zero energy in a two-color laser field (pink waveform in the lower left). Vertical blue and half-as-long vertical red arrows indicate photons with 400- and 800-nm wavelength, respectively. ZPD and BSD denote zero photon dissociation and bond-softening dissociation, respectively. ZPD_{stR} indicates ZPD via a stimulated Raman scattering process proceeding only on the $1s\sigma_g$ potential energy curve of H_2^+, and $ZPD_{2p\sigma_u}$ denotes ZPD by transient population of the $2p\sigma_u$ curve via absorption of a 400-nm photon and later emission of an 800-nm photon.

opposite ends of the interaction chamber. More details on our experimental setup can be found in our previous publications [2,38,43,44].

Measured momentum distributions of protons observed along the laser polarization direction z for different pulses are shown in Fig. 2. For the single-color measurements [Figs. 2(a) and 2(b)] we clearly identify the well-known peaks associated with the dissociation at the one-photon and the two-photon crossings [20,21,27], usually called bond-softening dissociation (BSD) and above-threshold dissociation (ATD) [30,31] (cf. the labeling in the figures).

The momentum distributions in Figs. 2(a) and 2(b) show that there are almost no protons observed with momenta smaller than 4 a.u. for both the narrow-band 800- and 400-nm pulses alone. In contrast, Fig. 2(c) shows that if both pulses are overlapped in time and space, the yield of protons with very small energy dramatically increases. A similar but somewhat less pronounced increase is also observed when broadband pulses are used [red line in Fig. 2(a)]. Evidently, the dissociation process leading to these abundant near-zero-energy protons involves photons of distinctively different colors. This is clearly confirmed by the absence of the near-zero-energy protons in the narrow-band pulses and, even more clearly, by a cross-check measurement where the 800- and 400-nm pulses were applied with a time delay of about 100 fs such that both colors are supplied temporally separated [Fig. 2(c)]. What is the mechanism behind the appearance of the near-zero-energy protons in the two-color and broadband pulses?

To answer this question, let us discuss the possible dissociation pathways that can lead to protons with energy close to zero (cf. Fig. 1). Dissociation starts after the ionization step $H_2 \rightarrow H_2^+ + e^-$. Following the Franck-Condon principle,

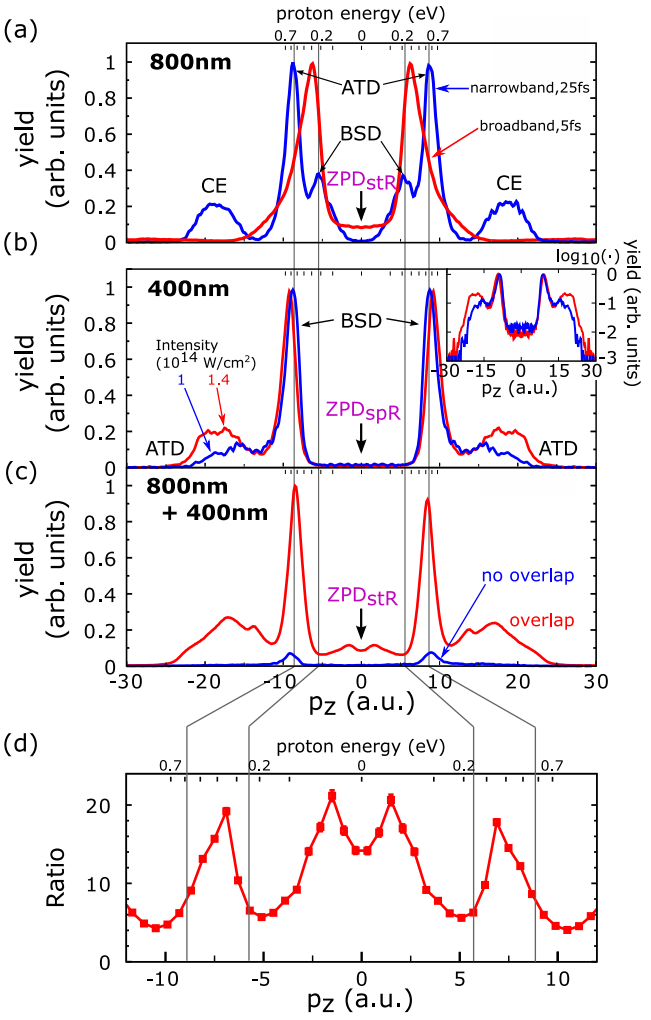

FIG. 2. Momentum distributions of protons along the laser polarization direction z. (a) Distributions measured with narrow-band pulses [FWHM bandwidth (BW) 50 nm around 800 nm, duration 25 fs] (blue line), in comparison with broadband laser pulses [FWHM BW roughly 300 nm around 740 nm, duration 5 fs] (red line), indicated by arrows, normalized to maximum. Intensities of both pulses are 2×10^{14} W/cm^2. CE, Coulomb explosion. (b) Distributions measured with narrow-band 400-nm pulses generated by frequency doubling (normalized) for two pulse peak intensities (in 10^{14} W/cm^2, encoded by colors and indicated by arrows). Inset: Same distributions on a logarithmic scale. (c) Distributions measured with two-color pulses (800 nm + 400 nm) for two cases: overlap of the two pulses, and separated in time (see text for details), as indicated by colors and arrows. Peak intensity is 1×10^{14} W/cm^2 for each color. (d) Ratio of yields taken from (c) between the cases with and without temporal overlap of the two pulses, normalized to the yield of H_2^+.

vibrational states around $v = 5$ will be dominantly populated in H_2^+ during ionization [24]. The dissociation barrier for $v = 5$ is about 1.6 eV. Thus, one 800-nm photon is not sufficient to populate vibrational states near the dissociation threshold. Contrarily, the energy of one 400-nm photon is large enough to populate such vibrational states and to cause dissociation via a ZPD process, in which a 400-nm photon is absorbed and a photon with lower energy is emitted by spontaneous Raman

scattering [28]. We abbreviate this zero-photon-dissociation process by ZPD_{spR}. However, the probability of the spontaneous Raman scattering process is notoriously small. The inset of Fig. 2(b) shows that for the 400-nm pulse we observe an accordingly small amount of protons with near-zero energy.

To explain the strong enhancement of the near-zero-energy proton yield in the two-color field [Fig. 2(c)], we propose that a *stimulated* Raman scattering process is at work. In this process, a high-lying vibrational state near the dissociation threshold is populated by the absorption of one 400-nm photon and the emission of one 800-nm photon (see the illustration in Fig. 1). Equivalent to the ZPD_{spR} mechanism, in this process also a net amount of zero photons is absorbed. However, the lower-energy photon is supplied by the second wavelength in the two-color pulse and, thus, this ZPD process becomes stimulated. We denote it by ZPD_{stR}. The strong enhancement of the (near-)zero-energy proton yield in the two-color field shown in Fig. 2(c) is therefore explained by the much higher cross section of the stimulated Raman process as compared to the spontaneous Raman scattering process. Analogously, we also ascribe the increase of the (near-)zero-energy proton yield observed with the broadband pulse [Fig. 2(a)] to ZPD_{stR} with photons from the red and blue wings of the spectrum. Although the photon energy difference from the red and blue wings is not sufficient to completely reach the dissociation threshold directly from $\nu = 5$, the stimulated Raman process can still take place from higher vibrational states. As these states are populated less probably during ionization, the yield enhancement for the (near-)zero-energy region is less pronounced than for the still more broadband two-color field. Nevertheless, this enhancement at very low energies is a clear sign of the action of the ZPD_{stR}, in accord with interpretations given in earlier work [40].

The ZPD_{stR} mechanism is fundamentally different from the $ZPD_{2p\sigma_u}$ mechanism described in, e.g., Refs. [15,29,37,39] and outlined above (cf. Fig. 1). The $ZPD_{2p\sigma_u}$ mechanism requires a transition from the $1s\sigma_g$ state to the $2p\sigma_u$ state of H_2^+. As the transition probabilities are largest when the two photons are resonant with these two states, this mechanism necessitates that the two photons are absorbed (respectively emitted) at two different internuclear distances. Therefore, it inevitably implies the involvement of nuclear motion and a delay between the absorption and emission steps. In contrast, the ZPD_{stR} mechanism only involves the $1s\sigma_g$ state and may happen directly within the Franck-Condon region without any nuclear motion.

The two processes, ZPD_{stR} and $ZPD_{2p\sigma_u}$, generate protons in slightly different kinetic energy ranges. Because ZPD_{stR} can, starting from around $\nu = 5$, reach the dissociation threshold, the kinetic energy of the protons can reach down to zero. $ZPD_{2p\sigma_u}$, in contrast, can only take place from higher vibrational levels that enable reaching internuclear distances where the 800-nm BSD process becomes available. As a result, $ZPD_{2p\sigma_u}$ leads to somewhat higher proton energies. Simulations and coincidence measurements performed in Ref. [39] show that the yield of protons produced by $ZPD_{2p\sigma_u}$ peaks around 100 meV and becomes negligibly small below 30 meV. This leveling off at this proton energy can be explained by the finite bandwidths of the laser pulses which inhibit a larger spread around the peak proton energy of 100 meV down to smaller energy values. In contrast, the ZPD_{stR} process can populate vibrational levels down to the dissociation threshold for both the two-color and broadband pulses. Even though in the latter case the process needs to start from higher ν (as explained above) due to the smaller energies of the blue spectral portion, the dissociation threshold is still reachable. Thus, the enhanced yield at (near-)zero energies visible in Fig. 2(a) constitutes evidence for the action of the stimulated Raman process.

Further evidence is obtained from the normalized ratio of the measured proton yields with and without overlap of the 800- and 400-nm pulses, shown in Fig. 2(d). Significant enhancement and suppression of the relative yields is observed at distinct values of the proton momentum. The enhancement around 7 a.u. ($\approx$360 meV) and the suppression at 10 a.u. ($\approx$700 meV) originate from the fact that in the two-color field dissociation via the absorption of three 800-nm photons and the emission of one 400-nm photon becomes possible [15]. These processes are not the primary subject of the present discussion. We are interested in the features at smaller momenta $|p_z| \lesssim 5$ a.u. ($\lesssim$185 meV). Take the dip at 5 a.u. This feature constitutes indirect evidence for the ZPD_{stR} process: Since ZPD_{stR} can happen directly in the Franck-Condon region, it depopulates the nuclear wave packet before it moves further along on the $1s\sigma_g$ state to reach the internuclear distance where BSD of 800 nm takes place. As a result, the 800-nm BSD process becomes suppressed resulting in the dip at 5 a.u. Direct evidence for the ZPD_{stR} process can be seen at $|p_z| \lesssim 3$ a.u. ($\lesssim$70 meV): As discussed above, the contributions from $ZPD_{2p\sigma_u}$ in this proton energy range are negligibly small [39] and only ZPD due to a Raman process can explain such low-energy protons [20]. Thus, the huge yield enhancement in comparison with the ZPD_{spR} process of the single-color 400-nm pulse shown in Fig. 2(d) verifies that the (near-)zero-energy protons are dominantly due to the ZPD_{stR} process.

Dissociation of H_2 in two-color fields may lead to notable $\Delta\varphi$-dependent up-down asymmetries in the proton yield, $A = (P_+ - P_-)/(P_+ + P_-)$, with P_+ the yield of protons ejected upwards ($p_z > 0$) and P_- the downwards proton yield ($p_z < 0$), as has been observed in many experiments, e.g., Refs. [1,5–7,15,16,45]. The usual explanation for the asymmetry in the low-energy region is wave-packet interference between dissociation on the $2p\sigma_u$ state (due to 800-nm BSD) and dissociation on the $1s\sigma_g$ state (due to the $ZPD_{2p\sigma_u}$). Now, having established that protons below about 30 meV are ejected dominantly along the ZPD_{stR} pathway while the two other pathways are significantly weaker, one should wonder about the origin of the asymmetry in this energy range. If one relatively stronger pathway interferes with two weaker ones, the result is not easily predictable. Indeed, we measure significantly smaller values for $A(\Delta\varphi, |p_z| < 5\,\text{a.u.})$ as compared to $A(\Delta\varphi, |p_z| > 5\,\text{a.u.})$, where more pathways are open [see Fig. 3(a)].

To understand how the asymmetry pattern $A(\Delta\varphi, |p_z| < 5\,\text{a.u.})$ is created one needs to look into the details of proton ejection in this momentum range. As we show, it is governed by the interplay of several processes. Figure 3(b) shows the momentum distributions of the protons as a function of $\Delta\varphi$. Two features are apparent: Their mean values, $\bar{p}_z$, vary

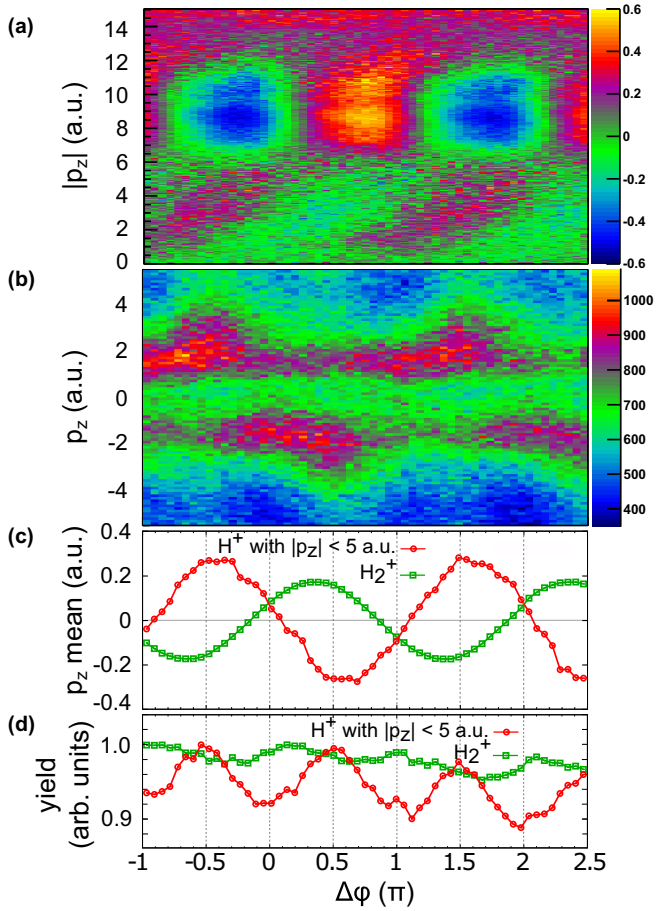

FIG. 3. (a) Asymmetry of proton emission (as defined in the text) as a function of $|p_z|$ over the relative phase $\Delta\varphi$ between 800- and 400-nm pulses. (b) Proton momentum distributions in the low-momentum region over $\Delta\varphi$. (c) Mean momentum values over $\Delta\varphi$ calculated for the distributions in (b) (red circles) and for H_2^+ (green squares). (d) Yields of protons from (b) (red circles) and for H_2^+ (green squares) over $\Delta\varphi$, both normalized at their respective maxima.

periodically with $\Delta\varphi$, and there is a $\Delta\varphi$-independent trench visible for $|p_z| \lesssim 1$ a.u. Obviously, the $\Delta\varphi$ oscillation of the spectra [$\bar{p}_z(\Delta\varphi)$ is shown by red circles in Fig. 3(c)] and their overlap with the trench is responsible for the observed asymmetry $A(\Delta\varphi, |p_z| < 5\,\text{a.u.})$, as the trench eats away the low-momentum parts of the spectra. One reason for the variation of $\bar{p}_z$ could be the center-of-mass (c.m.) recoil momentum that is imparted to H_2^+ during the ionization step, according to $p_z^{H_2^+} = p_z^{\text{c.m.}}(\Delta\varphi) = A_z(t_i, \Delta\varphi)$, where A_z is the laser vector potential along the z direction and t_i the instant of ionization. In a two-color field, $p_z^{\text{c.m.}}(\Delta\varphi)$ oscillates with $\Delta\varphi$ [38,46,47] [see the green squares in Fig. 3(c)]. However, Fig. 3(c) shows that the oscillations of $p_z^{\text{c.m.}}$ and $\bar{p}_z$ are almost out of phase. Thus, the $\Delta\varphi$ variation of $\bar{p}_z$ cannot be attributed to the ionization step, but may rather be caused by the joint actions of the ZPD_{stR}, the 800-nm BSD, and the $\text{ZPD}_{2p\sigma_u}$ processes. In combination with the yield lost in the trench [see the red line Fig. 3(d)], which is minimized whenever $|\bar{p}_z(\Delta\varphi)|$ becomes large, this explains the $\Delta\varphi$-dependent variation of the asymmetry, $A(\Delta\varphi, |p_z| < 5\,\text{a.u.})$.

But what is the reason for the observation of this trench in Fig. 3(b) for $|p_z| \lesssim 1$ a.u.? This trench, visible also as the dip at zero energy in Fig. 2(c), is the signature of a suppressed dissociation probability for (near-)zero energies. Such suppression has been interpreted within the Floquet picture as VT or bond hardening on the upper LIP of the zero- or one-photon dissociation branch (see, e.g., Refs. [25–29,34]). In this picture, VT can be considered the direct counterpart of the ZPD and BS processes. Other work has interpreted such suppression as the consequence of wavelength-dependent weak dipole coupling strengths of certain vibrational states [36]. With the ZPD_{stR} process introduced here, another possible explanation for the trapping enters the debate. Definite answers on the origins of trapping are beyond the scope of the current paper. However, we would like to point out that the above-discussed $\Delta\varphi$-dependent modulation of the trapped yield that shows maxima when the center of the momentum distributions overlaps with the trench (e.g., at $\Delta\varphi = 0$ or π) [cf. red dots in Fig. 3(d)] may be exploited by future work to obtain further insight into the dynamics leading to dissociation suppression.

In conclusion, we introduced experimental results on the dissociation of H_2^+ which we interpret as evidence for a stimulated Raman-scattering-based zero-photon-dissociation process, ZPD_{stR}. This process becomes active in the (near-) zero proton energy region whenever the bandwidth of the laser light is sufficient to cover the energy gap to the dissociation threshold. This ZPD_{stR} process introduced here can explain the strong proton yield enhancement in the near-zero-energy region observed in many two-color experiments and also in experiments [12,13] and simulations [24] with broadband few-cycle laser pulses centered around 730–750 nm. We furthermore show that the laser-field-induced asymmetry of H_2^+ dissociation in the (near-)zero-energy region is due to the combined action of several processes rather than only pathway interferences, with bond hardening taking a particularly important role. This finding opens up possibilities for detailed investigations of vibrational trapping and the influence of rotational states in molecular dynamics [33–35].

This work was financed by the Austrian Science Fund (FWF), Grants No. P21463-N22, No. P25615-N27, No. P28475-N27, and No. P30465-N27. F.H. was supported by the Innovation Program of Shanghai Municipal Education Commission (Grant No. 2017-01-07-00-02-E00034) and Shanghai Shuguang Project (No. 17SG10).

[1] M. F. Kling, P. von den Hoff, I. Znakovskaya, and R. de Vivie-Riedle, Phys. Chem. Chem. Phys. **15**, 9448 (2013).

[2] X. Xie, K. Doblhoff-Dier, S. Roither, M. S. Schöffler, D. Kartashov, H. Xu, T. Rathje, G. G. Paulus, A. Baltuška, S. Gräfe, and M. Kitzler, Phys. Rev. Lett. **109**, 243001 (2012).

[3] A. Alnaser, M. Kübel, R. Siemering, B. Bergues, N. G. Kling, K. Betsch, Y. Deng, J. Schmidt, Z. Alahmed, A. Azzeer, J. Ullrich, I. Ben-Itzhak, R. Moshammer, U. Kleineberg, F. Krausz, R. de Vivie-Riedle, and M. Kling, Nat. Commun. **5**, 3800 (2014).

[4] M. Kübel, R. Siemering, C. Burger, N. G. Kling, H. Li, A. S. Alnaser, B. Bergues, S. Zherebtsov, A. M. Azzeer, I. Ben-Itzhak, R. Moshammer, R. de Vivie-Riedle, and M. F. Kling, Phys. Rev. Lett. **116**, 193001 (2016).

[5] A. S. Alnaser and I. V. Litvinyuk, J. Phys. B: At. Mol. Opt. Phys. **50**, 032002 (2017).

[6] B. Sheehy, B. Walker, and L. F. DiMauro, Phys. Rev. Lett. **74**, 4799 (1995).

[7] M. R. Thompson, M. K. Thomas, P. F. Taday, J. H. Posthumus, A. J. Langley, L. J. Frasinski, and K. Codling, J. Phys. B: At. Mol. Opt. Phys. **30**, 5755 (1997).

[8] M. F. Kling, C. Siedschlag, A. J. Verhoef, J. I. Khan, M. Schultze, T. Uphues, Y. Ni, M. Uiberacker, M. Drescher, F. Krausz, and M. J. J. Vrakking, Science **312**, 246 (2006).

[9] M. Kremer, B. Fischer, B. Feuerstein, V. L. B. de Jesus, V. Sharma, C. Hofrichter, A. Rudenko, U. Thumm, C. D. Schröter, R. Moshammer, and J. Ullrich, Phys. Rev. Lett. **103**, 213003 (2009).

[10] B. Fischer, M. Kremer, T. Pfeifer, B. Feuerstein, V. Sharma, U. Thumm, C. D. Schröter, R. Moshammer, and J. Ullrich, Phys. Rev. Lett. **105**, 223001 (2010).

[11] I. Znakovskaya, P. von den Hoff, G. Marcus, S. Zherebtsov, B. Bergues, X. Gu, Y. Deng, M. J. J. Vrakking, R. Kienberger, F. Krausz, R. de Vivie-Riedle, and M. F. Kling, Phys. Rev. Lett. **108**, 063002 (2012).

[12] N. G. Kling, K. J. Betsch, M. Zohrabi, S. Zeng, F. Anis, U. Ablikim, B. Jochim, Z. Wang, M. Kübel, M. F. Kling, K. D. Carnes, B. D. Esry, and I. Ben-Itzhak, Phys. Rev. Lett. **111**, 163004 (2013).

[13] H. Xu, J. P. MacLean, D. E. Laban, W. C. Wallace, D. Kielpinski, R. T. Sang, and I. V. Litvinyuk, New J. Phys. **15**, 023034 (2013).

[14] H. Xu, T.-Y. Xu, F. He, D. Kielpinski, R. T. Sang, and I. V. Litvinyuk, Phys. Rev. A **89**, 041403(R) (2014).

[15] D. Ray, F. He, S. De, W. Cao, H. Mashiko, P. Ranitovic, K. P. Singh, I. Znakovskaya, U. Thumm, G. G. Paulus, M. F. Kling, I. V. Litvinyuk, and C. L. Cocke, Phys. Rev. Lett. **103**, 223201 (2009).

[16] H. Xu, H. Hu, X.-M. Tong, P. Liu, R. Li, R. T. Sang, and I. V. Litvinyuk, Phys. Rev. A **93**, 063416 (2016).

[17] V. Wanie, H. Ibrahim, S. Beaulieu, N. Thiré, B. E. Schmidt, Y. Deng, A. S. Alnaser, I. V. Litvinyuk, X.-M. Tong, and F. Légaré, J. Phys. B: At. Mol. Opt. Phys. **49**, 025601 (2016).

[18] A. Giusti-Suzor, F. H. Mies, L. F. DiMauro, E. Charron, and B. Yang, J. Phys. B: At. Mol. Opt. Phys. **28**, 309 (1995).

[19] J. H. Posthumus, Rep. Prog. Phys. **67**, 623 (2004).

[20] P. H. Bucksbaum, A. Zavriyev, H. G. Muller, and D. W. Schumacher, Phys. Rev. Lett. **64**, 1883 (1990).

[21] A. Zavriyev, P. H. Bucksbaum, H. G. Muller, and D. W. Schumacher, Phys. Rev. A **42**, 5500 (1990).

[22] A. Giusti-Suzor, X. He, O. Atabek, and F. H. Mies, Phys. Rev. Lett. **64**, 515 (1990).

[23] J. McKenna, A. M. Sayler, F. Anis, B. Gaire, N. G. Johnson, E. Parke, J. J. Hua, H. Mashiko, C. M. Nakamura, E. Moon, Z. Chang, K. D. Carnes, B. D. Esry, and I. Ben-Itzhak, Phys. Rev. Lett. **100**, 133001 (2008).

[24] J. McKenna, F. Anis, A. M. Sayler, B. Gaire, N. G. Johnson, E. Parke, K. D. Carnes, B. D. Esry, and I. Ben-Itzhak, Phys. Rev. A **85**, 023405 (2012).

[25] A. Giusti-Suzor and F. H. Mies, Phys. Rev. Lett. **68**, 3869 (1992).

[26] A. Zavriyev, P. H. Bucksbaum, J. Squier, and F. Saline, Phys. Rev. Lett. **70**, 1077 (1993).

[27] L. J. Frasinski, J. H. Posthumus, J. Plumridge, K. Codling, P. F. Taday, and A. J. Langley, Phys. Rev. Lett. **83**, 3625 (1999).

[28] J. H. Posthumus, J. Plumridge, L. J. Frasinski, K. Codling, E. J. Divall, A. J. Langley, and P. F. Taday, J. Phys. B: At. Mol. Opt. Phys. **33**, L563 (2000).

[29] B. Moser and G. N. Gibson, Phys. Rev. A **80**, 041402(R) (2009).

[30] H. Ibrahim, C. Lefebvre, A. D. Bandrauk, A. Staudte, and F. Légaré, J. Phys. B: At. Mol. Opt. Phys. **51**, 042002 (2018).

[31] H. Li, X. Gong, K. Lin, R. de Vivie-Riedle, X. M. Tong, J. Wu, and M. F. Kling, J. Phys. B: At. Mol. Opt. Phys. **50**, 172001 (2017).

[32] M. Šindelka, N. Moiseyev, and L. S. Cederbaum, J. Phys. B: At. Mol. Opt. Phys. **44**, 045603 (2011).

[33] G. J. Halász, Á. Vibók, M. Šindelka, N. Moiseyev, and L. S. Cederbaum, J. Phys. B: At. Mol. Opt. Phys. **44**, 175102 (2011).

[34] P. Badankó, G. J. Halász, and Á. Vibók, Sci. Rep. **6**, 31871 (2016).

[35] A. Natan, M. R. Ware, V. S. Prabhudesai, U. Lev, B. D. Bruner, O. Heber, and P. H. Bucksbaum, Phys. Rev. Lett. **116**, 143004 (2016).

[36] J. McKenna, F. Anis, B. Gaire, N. G. Johnson, M. Zohrabi, K. D. Carnes, B. D. Esry, and I. Ben-Itzhak, Phys. Rev. Lett. **103**, 103006 (2009).

[37] X. Gong, P. He, Q. Song, Q. Ji, H. Pan, J. Ding, F. He, H. Zeng, and J. Wu, Phys. Rev. Lett. **113**, 203001 (2014).

[38] X. Xie, S. Roither, D. Kartashov, L. Zhang, A. Baltuška, and M. Kitzler, High Power Laser Sci. Eng. **4**, e40 (2016).

[39] W. Zhang, H. Li, K. Lin, P. Lu, X. Gong, Q. Song, Q. Ji, J. Ma, H. Li, H. Zeng, F. He, and J. Wu, Phys. Rev. A **96**, 033405 (2017).

[40] B. Gaire, Ph.D. thesis, Kansas State University, 2011.

[41] R. Dörner, V. Mergel, O. Jagutzki, L. Spielberger, J. Ullrich, R. Moshammer, and H. Schmidt-Böcking, Phys. Rep. **330**, 95 (2000).

[42] J. Ullrich, R. Moshammer, A. Dorn, R. Dörner, L. P. H. Schmidt, and H. Schmidt-Böcking, Rep. Prog. Phys. **66**, 1463 (2003).

[43] L. Zhang, X. Xie, S. Roither, D. Kartashov, Y. L. Wang, C. L. Wang, M. Schöffler, D. Shafir, P. B. Corkum, A. Baltuška, I. Ivanov, A. Kheifets, X. J. Liu, A. Staudte, and M. Kitzler, Phys. Rev. A **90**, 061401(R) (2014).

[44] X. Xie, T. Wang, S. G. Yu, X. Y. Lai, S. Roither, D. Kartashov, A. Baltuška, X. J. Liu, A. Staudte, and M. Kitzler, Phys. Rev. Lett. **119**, 243201 (2017).

[45] J. Wu, M. Magrakvelidze, L. P. H. Schmidt, M. Kunitski, T. Pfeifer, M. Schöffler, M. Pitzer, M. Richter, S. Voss, H. Sann, H. Kim, J. Lower, T. Jahnke, A. Czasch, U. Thumm, and R. Dörner, Nat. Commun. **4**, 2177 (2013).

[46] X. Xie, S. Roither, D. Kartashov, E. Persson, D. G. Arbó, L. Zhang, S. Gräfe, M. S. Schöffler, J. Burgdörfer, A. Baltuška, and M. Kitzler, Phys. Rev. Lett. **108**, 193004 (2012).

[47] X. Xie, S. Roither, S. Gräfe, D. Kartashov, E. Persson, C. Lemell, L. Zhang, M. S. Schöffler, A. Baltuška, J. Burgdörfer, and M. Kitzler, New J. Phys. **15**, 043050 (2013).